Evaluation of several WRF/NMM-CMAQ vertical coupling configurations

Pius Lee*, Marina Tsidulko, Hui-Ya Chuang
Scientific Applications International Corporation, Beltsville, MD.

Hsin-Mu Lin, Daiwen Kang
Science and Technology Corporation, Hampton, VA

Jeff McQueen, Tom Black, Geoff DiMego
Mesoscale Modeling Branch
NOAA/NWS/NCEP/Environmental Modeling Center, Camp Springs, MD

Rohit Mathur, Jon Pleim, George Pouliot, Tanya Otte, Jeff Young, David Wong, Ken Schere
NOAA/ARL/Atmospheric Sciences Modeling Division, RTP, NC
(On assignment to the EPA/National Exposure Research Laboratory)

Nelson Seaman and Paula Davidson
NOAA/NWS/Office of Science and Technology, Silver Spring, MD

1. INTRODUCTION

During 2003, NOAA and the U.S. EPA signed a Memorandum of Agreement to work together to develop a National air quality forecasting capability. To meet this goal, NOAA's National Weather Service (NWS), the Office of Atmospheric Research (OAR) and the U.S. EPA developed and evaluated a prototype ozone forecast capability for the North Eastern U.S. (Davidson et al. 2004). Subsequently, a national Air Quality Forecast System (AQFS) was envisioned comprising the NWS/National Centers for Environmental Prediction (NCEP) North American Model (NAM) model at 12 km (Janic 2003) to provide meteorological predictions for the EPA Community Multi-scale Air Quality (CMAQ) model (Bynn and Ching 1999) to produce up to 48-h ozone predictions for Northeastern U.S. This capability, often referred to as the Initial Operational Capability (IOP) of AQFS was officially declared operational by the Weather Service in September 2004. The capability of AQFS was officially expanded to cover an enlarged geographically domain covering Eastern U.S. in September 2005 (McQueen et al. 2007).

In the interim of this latest official upgrade of AQFS and the end of the 2006 ozone season, a major upgrade of the vertical coupling scheme between the met model and the chemistry models of the system is being tested in developmental mode (Lin et al. 2006). The CMAQ model used in this developmental version of CMAQ used in this study is closely abided to CMAQ-4.5. It is configured with Asymmetric Convective Model for in-cloud convective mixing (Pleim 2006), NAM derived radiative field for photolysis attenuation calculation, and static boundary conditions for all chemical constituents. The following sections summarize the methodology, qualitative and quantitative verification, and analysis of the impact of potential refinement of the upgrade, respectively.

2. VERTICAL COUPLING SCHEMES

CMAQ uses a generalized vertical co-ordinate system (Bynn and Ching 1999). This allows flexibility for the user to devise a variety of vertical structures as long as a corresponding set of transformation Jacobians between the physical space and the computational space is also provided. Boundary and initial conditions are customarily given in computational space. In this study two paradigms of vertical structure have been considered. The former is referred as the “loose” scheme as CMAQ, unlikely using NAM’s hybrid co-ordinate as shown in Fig. 1a, is prescribed to use a terrain following σ-p co-ordinate. Therefore, vertical interpolations are required. The latter is referred as the “tight” scheme as CMAQ is adopting a hybrid co-ordinate system based on the one used by NAM.

2.1 The Loose Scheme

In the operational version of AQFS, NAM feeds CMAQ with meteorological and surface characteristic fields in terrain-following σ surfaces (Otte et al 2005). The version uses 22 σ layers as shown in Fig. 1b. The data flow between NAM and CMAQ is achieved through the processing of two interface processors: WRF/NMM-Post and AQFS-Prdgen as schematically shown in Fig. 2. WRF/NMM-Post does the layer collapsing operation by vertically interpolating met fields from NAM's hybrid full-levels to the sigma levels used in CMAQ basing on atmospheric pressure. All met fields are on mid σ levels except that vertical diffusivity, K_z, is staggered on full σ levels. Upon the completion of WRF/NMM-Post, AQFS-Prdgen is convoked to perform horizontal interpolation to map the NAM output in Arakawa E staggered grid with rotated latitude-longitude map projection (Black 1994) onto CMAQ's Arakawa C grid with Lambert secant conformal map projection.

2.2 The Tight Scheme

In the developmental version of AQFS, NAM feeds CMAQ with meteorological and surface fields in a "pressure for upper levels and terrain following σ-p for lower levels" hybrid vertical co-ordinate system as shown in Fig 1a. NAM uses 61 full levels. Level 42 is the transition level with its pressure lies at around 420 hPa, dynamically determined dependent on the terrain and the instantaneous vertical air motion in the column (Janic 2003). The tight coupling scheme adopts the same hybrid structure for the CMAQ model except that not all 61 levels in NAM are used. A "pick and choose" procedure basing on heuristically maximizing fidelity of the meteorology is used to select a subset of these 61 levels. In this study two such selections of levels to build hybrid co-ordinate systems for the CMAQ model have been attempted. These attempts comprised the two latter cases of a set of sensitivity study. They are referred to as the 22-tight and 29-tight cases, respectively. In essence, the tight coupling scheme avoids the vertical interpolation step in WRF/NMM-Post. Nonetheless, the AQFS-Prdgen steps mentioned above in the loose coupling scheme are still needed here for horizontal grid mappings.

3. SENSITIVITY CASES: AUGUST 2-4, 2006

There were a few of elevated surface O3 concentration scenarios in many cities in Eastern U.S. between August 2 and 4, 2006. Figure 3a shows the 1 h daily maximum concentration for August 3 compiled by the AIRNOW observation network (EPA 2006). It can be noticed that there were areas with 1 h daily max value in excess of 100 ppb; namely in the San Francisco Bay Area, Central Valley and Los Angeles Basin in California; near Charlotte, South Carolina; Philadelphia, Pennsylvania; and Long Island, New York.

This study included 3 runs of the developmental version of AQFS to reconstruct the August 3 scenario. Table 1 summarizes the nomenclature and a brief description of the cases. All three cases were daily 12Z cycle 48h free forecasts initialized at 12Z August 1st, 2006.

Table 1 Run cases include in the sensitivity study

Case	Main distinctive feature of CMAQ model
LS	Loose vertical coupling as described in Section 2.1 with 22 σ-p layers (Fig. 1b)
TG-22	Tight vertical coupling as described in Section 2.2 with 22 hybrid layers.
TG-29	Same as TG-22 but for 29 layers.

The TG-22 case "pick-and-chose" full hybrid levels 1, 2, 4, 6, 8, 10, 12, 14, 16, 18, 20, 22, 25, 28, 31, 34, 37, 41, 43, 46, 49, 53, and 57 from the NAM model's 61 full levels, totaling 23 chosen levels. The met fields are then interpolated to its corresponding mid levels, totaling 22 mid-levels, to drive the CMAQ model.

A similar procedure was used to derive met fields from NAM to the TG-29 case, except that finer vertical resolution has been introduced by inserting 7 net layers, namely: by adding levels 3, 5, 24, 26, 30, 32, 45, 47, 51, and 55, but deleting levels 25, 31, and 46. The additional resolutions are placed at heights likely to capture characteristics of near surface dynamics, shallow convection above mid afternoon PBL, and stratospheric intrusion of O3 at the tropopause.

4. O3 FORECAST ON AUGUST 3, 2006

The daily maximum temperature on August 3rd, 2006 over the Continental U.S. was high with large swath area in Eastern U.S. exceeding 37°C. The high temperatures was already ebbing on that day after a 3 day heat wave started on August 1st. As discussed in Section 3, many cities across Eastern U.S. had code orange or code red O3 day on August 3rd. Figure 3b showed forecast results from the TG-22 case

verified with AIRNOW data. The forecast captured exceedances in New England; and Charlotte, South Carolina areas, but missed those in California. This pattern is common to all three cases. Figures 4 and 5 show the difference maps between TG-22 and LS, and TG-22 and TG-29, respectively.

4.1 Spatial verification

TG-22 verifies better than LS, as large swath of area in the states of Utah and Arizona showed marked improvement by TG-22 over LS. LS tended to overestimated PBL height due to vertical interpolation in the WRF/NMM-Post step. In that part of the country, mid-afternoon PBL height can be several km high. As the upper troposphere always present itself as a potent source of intruded stratospheric O3, the tall PBL can tap into this pool of source of O3. The overshoot of PBL calculation in the LS case resulted in aggravation of over prediction of surface O3. It is believed that with the elimination of the interpolation step, TG-22 reduced the daily hourly bias in both mid afternoon and mid night by several ppb in this region. Figures 6-8 show the spatial verification maps of cases LS, TG-22, and TG-29 respectively.

4.2 Categorical Statistics verification

Basing on a skill score metric used routinely at U.S. EPA (e.g., Kang et al. 2005) the following set of criteria to rank forecast score is used[1]: Accuracy (*A*) is the percentage of forecasts that correctly predict exceedances and non-exceedances. Accuracy is strongly influenced by the number of correctly forecast nonexceedances which is invariably rather large; hence, care must be taken in its interpretation. A perfect score is 100%.

$$A = \left(\frac{b+c}{a+b+c+d} \right) \cdot 100\% \qquad (1)$$

Bias (*B*) indicates whether a forecast tends to err in over-prediction (false positives) or in under-prediction (false negatives). A value of 1 indicates no bias; values below 1 indicate under-prediction and above 1 indicate over-prediction.

$$B = \left(\frac{a+b}{b+d} \right) \qquad (2)$$

The false alarm ratio (*FAR*) is a measure of the percentage of forecast exceedances that did not verify. A perfect score is 0%.

$$FAR = \left(\frac{a}{a+b} \right) \cdot 100\% \qquad (3)$$

The probability of detection (*POD*), or "hit rate", indicates which percentage of observed exceedances were correctly forecast. *POD* focuses on observations only. *POD* could be close to 100%, i.e., a perfect score, for a system with a large over-prediction, i.e., a large *a*.

$$POD = \left(\frac{b}{b+d} \right) \cdot 100\% \qquad (4)$$

The critical success index (*CSI*) measures the correspondence between forecast and observed exceedance events. Therefore, *CSI* measures both observed and forecast exceedences and how these exceedences were matched as indicated by *b*. *CSI* may be considered as a joint measure of *POD* and *FAR*. A perfect score is 100%.

$$CSI = \left(\frac{b}{a+b+d} \right) \cdot 100\% \qquad (5)$$

Table 2 Categorical Statistics of sensitivity runs

	LS	TG-22	TG-29
A	98.40	98.49	
B	1.65	1.25	
FAR	77.2	55	
POD	10.9	10.9	
CSI	8.08	8.64	
a	19	16	
b	8	8	
c	3224	3227	
d	34	34	

Table 2 show that, basing on FAR and POD, the TG-22 and TG-29 are doing just as well as LS in correctly forecasting an exceedance event at a less expense of FAR.

5. LONG ISLAND PLUME PROFILES

[1] Figure 9 shows a scatter plot where *a*, *b*, *c*, and *d* conveniently equal the number of data points falling within the four different regions of the diagram. The threshold value defining exceedance is 85 ppb for the daily maximum 8-h average ozone mixing ratio.

During the high surface O3 concentration episode, a large swath of area offshore the Long Island Sound experienced high surface O3 concentration. All the three sensitivity cases verified rather well for the daily 1 h max over the nearby maritime AIRNOW stations. Therefore a degree of confidence can be placed on the fidelity of these forecast in this area, especially during the mid afternoon peak O3 scenarios. Although they also captured this offshore plume rather similarly, slight variations were exhibited. It is thus interesting to investigate the vertical concentration profiles of some of the gaseous species to infer the impact of the various vertical coupling schemes on transport and transformation of the precursors and products of a pollution plume.

Figures 10a-c show the forecast vertical concentration profiles of O3 along a West to East cross section of about 450 km wide, passing New York City for the 3 cases at 3:00 pm local time on August 3rd, 2006. Similarly, Figs. 10 d-f show those for 3:00 am on August 4. Figure 11 displays the same information as Fig. 10, but for CO. The snap shots are likely to capture the highest intensity of the land and sea breeze circulation at its afternoon and early morning peaks. In the mid afternoons the low level flows were predominately North-westerly; whereas in the early mornings South-easterly flows prevailed.

The co-ordinate axis of these profile plots are evenly spaced according to level indices. Therefore the compounded thickness between levels 1 and 14 is about 2 km. The upper-most layer thickness is about 4 km.

Figures 10a-c shows that in the mid afternoon of August 3, thermal convection has brought O3 to an attitude around 2 km, the top of PBL, at around 80 km down wind of New York City. Spatially speaking, the O3 plume remained contiguous for more than 100 km maintaining its single concentration maximum near surface. On the contrary at 3:00 am, as shown in figures 10d-f, return flow of the land-sea breeze produced a secondary concentration maximum aloft at around 1.5 km attitude 30 km inland of the City. These features were also observed for CO in Fig. 11.

Comparing the profiles of the 3 sensitivity cases, an overarching similarity is obvious. The subtle difference between those of TG-22 and TG-29 is worth noting, as they were constructed with the same coupling paradigm while the latter had refinement at the three attitudes where atmospheric dynamics is believed to influence O3 forecast.

6. SUMMARY

A sensitivity study on a recent high surface O3 concentration episode has been performed to investigate the impact of various vertical coupling schemes between the met and chemistry models of the developmental version of the national Air Quality Forecast System. A loose coupling and a tight coupling paradigm have been attempted. The tight coupling scheme is believed to be more promising as less interpolation is involved in ingest of the met fields. It also provide better flexibility of fine tuning vertical resolution at the attitude of interest as has been demonstrated in this study.

ACKNOWLEDGEMENTS

The views expressed are those of the authors and do not necessarily represent those of the National Weather Service, NOAA or the EPA. EPA AIRNOW program staff provided the observations necessary for quantitative model evaluation.

REFERENCES

Byun, D. W., and J. K. S. Ching (Eds.), 1999: Science algorithms of the EPA Models-3 Community Multiscale Air Quality (CMAQ) Modeling System. EPA-600/R-99/030, Office of Research and Development, U.S. Environmental Protection Agency, Washington, D.C. [Available from U.S. EPA, ORD, Washington, D.C. 20460.]

Davidson, P.M., N. Seaman, K. Schere, R.A. Wayland, J.L. Hayes and K.F. Carey, 2004: National Air Quality Forecasting Capability: First Steps toward Implementation. Preprints, 6th Conference on Atmospheric Chemistry: Air Quality in Megacities. Seattle, WA, Jan 11-15, 2004.

EPA, cited 2006: 2006 summer ozone season – Archive. [Available online at http://www.airnow.gov/index.cfm?action=airnow.archivescalendar

Janjic, Z.I., 2003: A nonhydrostatic model based on a new approach, *Meteorol. Atmos. Phys.*, **82**, 271-285.

Kang, D., B. K. Eder, A. F. Stein, G. A. Grell, S. E. Peckham, and J. McHenry, 2005: The New England air quality forecasting pilot program: Development of an evaluation protocol and performance benchmark. *J. Air & Waste Manage. Assoc.*, **55**, 1782-1796.

Lin H. M., P. Lee, and H.Y. Chuang, 2006: Direct linkage of meteorological data for WRF-NMM/CMAQ Coupling. Preprints, *8th Conference on Atmospheric Chemistry*: Atlanta, GA, Jan 2006.

McQueen, J., P. Lee, M. Tsidulkp, S. Lu, G. DiMego, P. Davidson, and N. Seaman, 2007: Update to and Recent Performance of the NAM-CMAQ Modeling system at NCEP operations, Preprints, *9th Conference on Atmospheric Chemistry*, San Antonio, TX, Amer. Meteor. Soc., Jan, 2007.

Otte, T. L., G. Pouliot, J. E. Pleim, J. O. Young, K. L. Schere, D. C. Wong, P.C. Lee, M. Tsidulko, J. T. McQueen, P. Davidson, R. Mathur, H. Y. Chuang, G. DiMego, and N. Seaman, 2005: Linking the Eta Model with the Community Multiscale Air Quality (CMAQ) modeling system to build a national air quality forecasting system. *Wea. Forecasting*, **20**, 367-384.

Pleim, J.E., 2006: A new combined local and non-local PBL model for meteorological and air quality modeling. This preprint. *5th Annual CMAS Conference*, Chapel Hill, NC, October 2006.

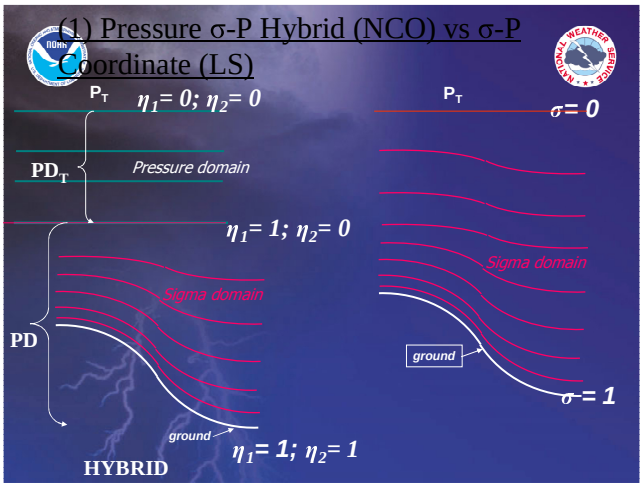

Figure 1 Vertical grid strurcture (a) Hybrid, and (b) Terrain following σ-p

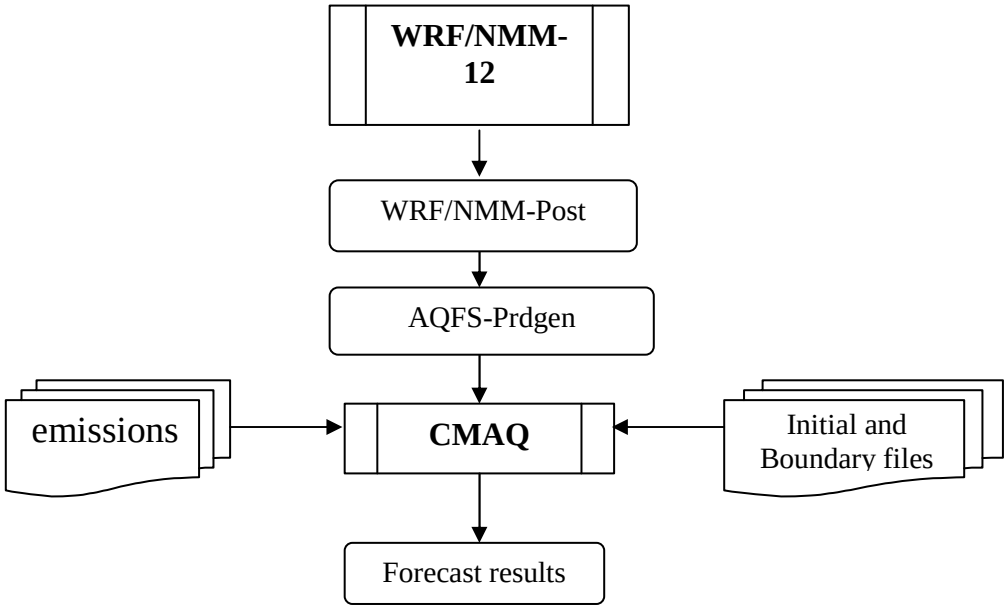

Figure 2. Data flow of the WRF/NMM-12 and CMAQ coupled modeling system

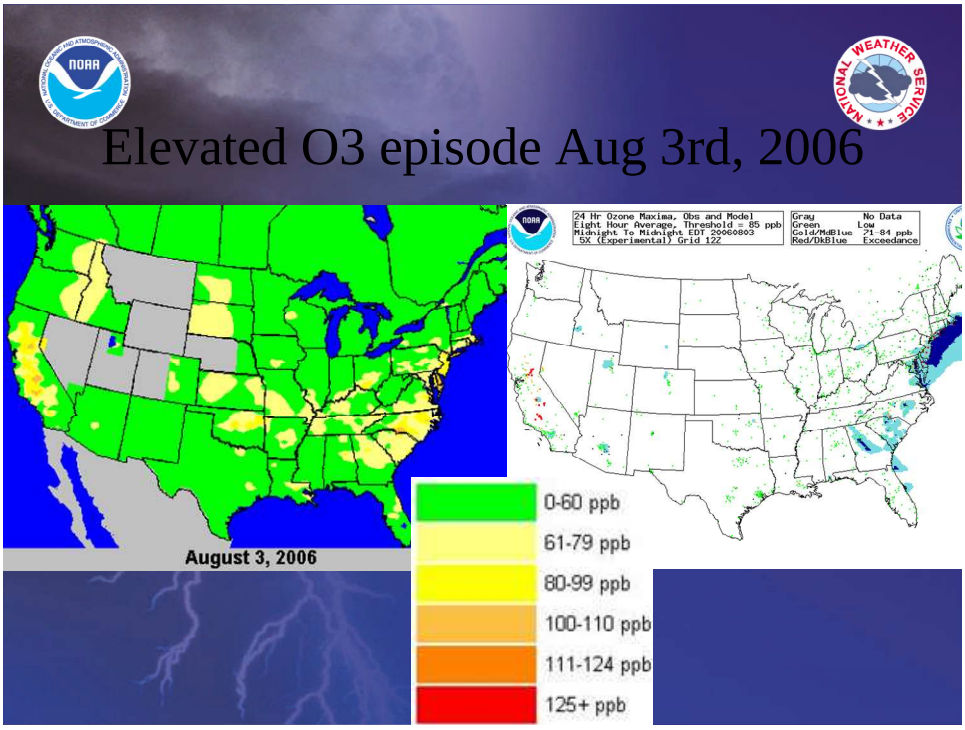

Fig. 3 Daily maximum hourly surface O3 concentration on August 3, 2006 (a) Observed by AIRNOW, and (b) Forecasted by the TG-22 case verified with AIRNOW data

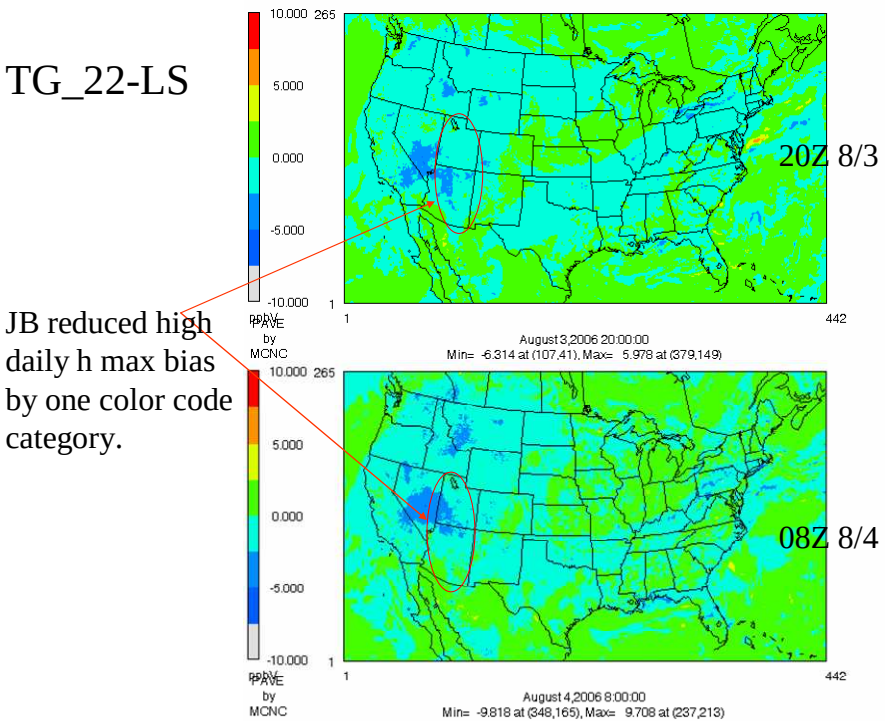

Fig. 4 Difference map for forecast surface O3 concentration between TG-22 and LS

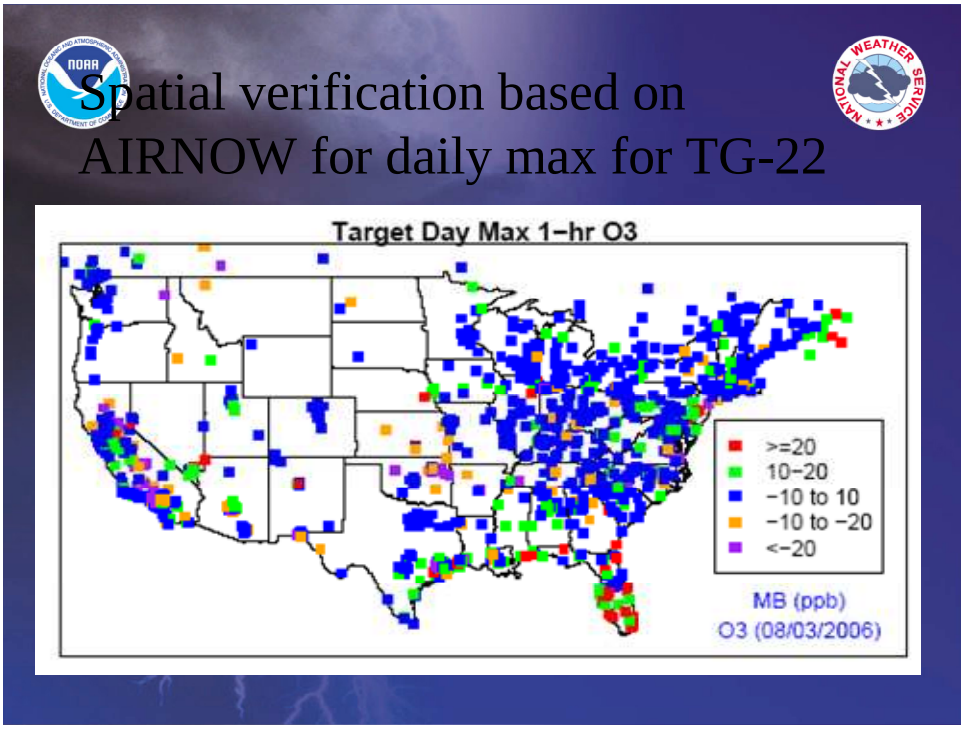

Fig. 6 Spatial verification map for daily hourly maximum surface O3 concentration with AIRNOW data for the TG-22 case for the August 3rd, 2006 forcast initialized at 12Z August 2nd, 2006.

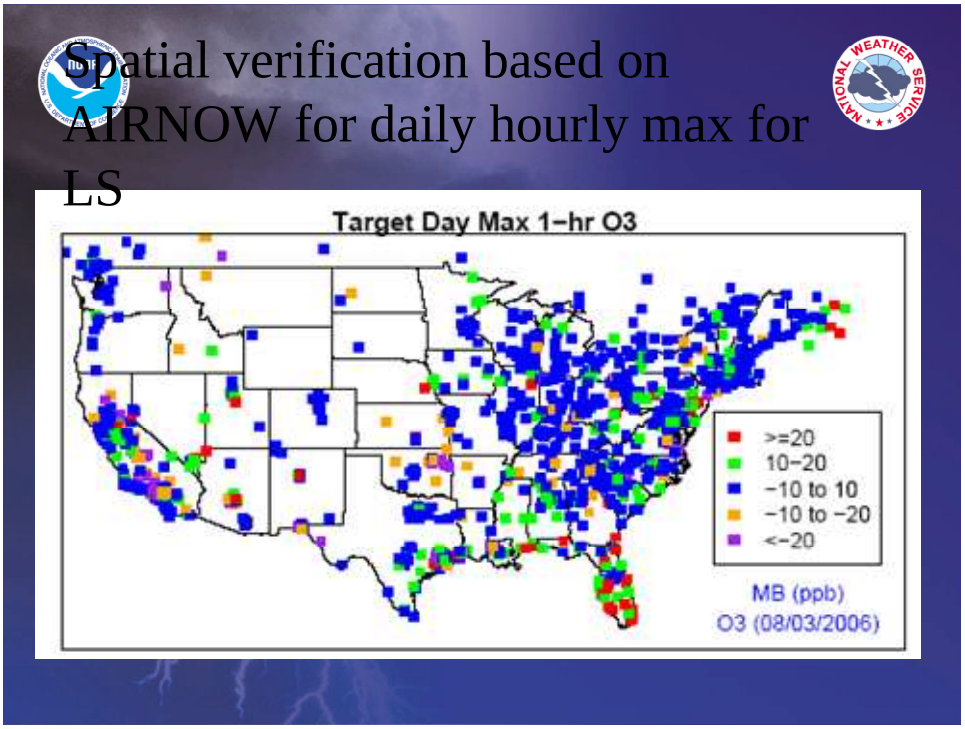

Fig. 7 Spatial verification map for daily hourly maximum surface O3 concentration with AIRNOW data for the LS case for the August 3rd, 2006 forcast initialized at 12Z August 2nd, 2006.

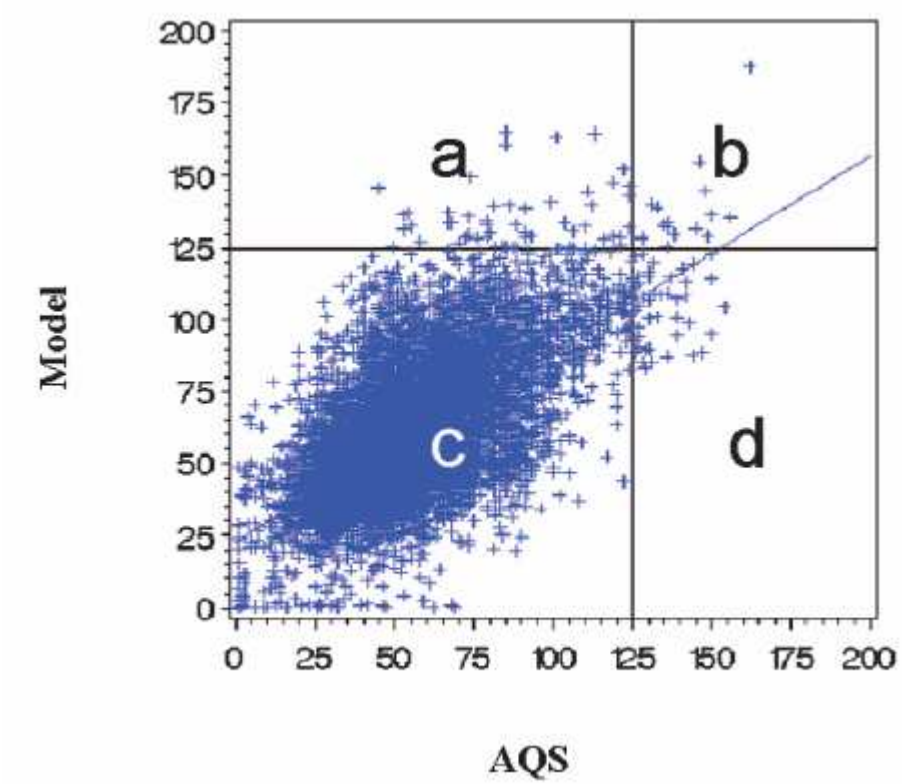

Fig. 9 Sample scatter plot depicting the definition of the regions: a,b,c and d for categorical evaluation